The AAA-ATPase p97 facilitates degradation of apolipoprotein B by the ubiquitin-proteasome pathway[S]

Eric A. Fisher,[1] Louis R. Lapierre,[1] Robert D. Junkins, and Roger S. McLeod[2]

Department of Biochemistry and Molecular Biology, Dalhousie University, Halifax, Nova Scotia, Canada

Abstract **The ATPase associated with various cellular activities (AAA-ATPase) p97 (p97) has been implicated in the retrotranslocation of target proteins for delivery to the cytosolic proteasome during endoplasmic reticulum-associated degradation (ERAD). Apolipoprotein B-100 (apoB-100) is an ERAD substrate in liver cells, including the human hepatoma, HepG2. We studied the potential role of p97 in the ERAD of apoB-100 in HepG2 cells using cell permeabilization, coimmunoprecipitation, and gene silencing. Degradation was abolished when HepG2 cytosol was removed by digitonin permeabilization, and treatment of intact cells with the proteasome inhibitor MG132 caused accumulation of ubiquitinated apoB protein in the cytosol. Cross-linking of intact cells with the thiol-cleavable agent dithiobis(succinimidyl-propionate) (DSP), as well as nondenaturing immunoprecipitation, demonstrated an interaction between p97 and intracellular apoB. Small interfering ribonucleic acid (siRNA)-mediated reduction of p97 protein increased the intracellular levels of newly synthesized apoB-100, predominantly because of a decrease in the turnover of newly synthesized apoB-100 protein. However, although the posttranslational degradation of newly synthesized apoB-100 was delayed by p97 knockdown, secretion of apoB-100 was not affected. Knockdown of p97 also impaired the release of apoB-100 and polyubiquitinated apoB into the cytosol. In summary, our results suggest that retrotranslocation and proteasomal degradation of apoB-100 can be dissociated in HepG2 cells, and that the AAA-ATPase p97 is involved in the removal of full-length apoB from the biosynthetic pathway to the cytosolic proteasome.**—Fisher, E. A., L. R. Lapierre, R. D. Junkins, and R. S. McLeod. **The AAA-ATPase p97 facilitates degradation of apolipoprotein B by the ubiquitin-proteasome pathway.** ***J. Lipid Res.*** **2008.** 49: **2149–2160.**

Supplementary key words retrotranslocation • endoplasmic reticulum-associated degradation • ERAD • permeabilization • proteolysis

Apolipoprotein B-100 (apoB-100) is the major protein component of VLDLs. Hepatic assembly of VLDL is initiated in the endoplasmic reticulum (ER), where a primordial lipoprotein particle is formed. Following further lipidation, a mature triglyceride-rich apoB-containing lipoprotein (LpB) is transported through the secretory pathway and into the plasma (as reviewed in Refs. 1, 2). Several studies have demonstrated that a portion of newly synthesized apoB is subject to intracellular degradation and have suggested that hepatic LpB production may be regulated by multiple degradation mechanisms (as reviewed in Refs. 3, 4). Three degradation pathways have been described for different stages during apoB maturation: ER-associated degradation (ERAD), post-ER presecretory proteolysis (PERPP), and cell surface reuptake. The cytosolic ubiquitin-proteasome system and ER lumenal proteases have been implicated in apoB ERAD (5–7).

There is evidence in cultured rodent primary hepatocytes to suggest that ERAD (8), PERPP (9), and cell surface reuptake (10) have in vivo relevance in modulating LpB levels. In addition, cell culture studies using ritonavir, a protease inhibitor included in the anti-retroviral treatment for the human immunodeficiency virus, have suggested that this agent can modulate hepatic LpB secretion (11). Ritonavir inhibits the chymotrypsin-like activity of the proteasome (12), an activity particularly important in apoB degradation (7). Impaired proteasome function may explain the increased plasma levels of VLDL and hyperlipidemia in patients receiving anti-retroviral therapy.

The ubiquitin-proteasome system is a well-characterized pathway for the regulatory proteolysis of intracellular proteins involved in various cellular functions (as reviewed in Refs. 13, 14). The proteasome is a large multi-protein complex consisting of two subunits, a 20S proteolytic core complex capped by two 19S regulatory subunits. Regulatory subunits serve as the entry point for the delivery of substrate proteins to the proteolytic core. In the past 15 years, the mechanism by which the apoB polypeptide can become accessible to the ubiquitin-proteasome system has

This work was supported by the Canadian Institutes of Health Research, Grant MOP-67073, and by graduate scholarships from the Nova Scotia Health Research Foundation and the Walter C. Sumner Foundation (L.R.L.).

Manuscript received 28 February 2008 and in revised form 19 May 2008 and in re-revised form 5 June 2008.

Published, JLR Papers in Press, June 11, 2008.
DOI 10.1194/jlr.M800108-JLR200

[1] E. Fisher and L. Lapierre contributed equally to this work.
[2] To whom correspondence should be addressed.
e-mail: rmcleod2@dal.ca
[S] The online version of this article (available at http://www.jlr.org) contains supplementary data in the form of two figures.

been the subject of intense investigation. One prevalent hypothesis is that the translocation of the apoB polypeptide across the ER membrane may be at least temporarily arrested, as a result of the failure to efficiently assemble the nascent lipoprotein particle (15, 16). If translation proceeds without coupling to translocation, the nascent polypeptide chain can loop out of the translocation channel into the cytosol, making it accessible to components of the proteasomal degradation machinery. Cytosolic chaperones, including the heat shock proteins Hsp70 and Hsp90, have been suggested to play a role in apoB degradation by facilitating delivery of the apoB polypeptide to the proteasome (17). In addition, the tumor autocrine motility factor gp78, an E3 ubiquitin ligase, has been shown to play a role in apoB polyubiquitination (18). While E3 ligases and molecular chaperones are important factors in targeting an ERAD substrate to the proteasome, key components in the recognition and extraction of apoB from the ER to the cytosol have not yet been characterized.

Degradation of aberrant proteins by ERAD, or the failure thereof, has been linked to human disease (as reviewed in Refs. 19, 20). Studies in yeast, where ERAD was first described, have demonstrated that retrotranslocation (or dislocation) of ER lumenal and membrane-associated proteins to the cytosol is necessary for proteasomal degradation (21). Retrotranslocation in yeast involves several proteins associated with the ER membrane (as reviewed in Ref. 22), including adaptor proteins Npl4 and Ufd1 in complex with the hexamer of Cdc48p, an AAA-ATPase. Whereas Npl4 and Ufd1 have a role in ubiquitinated substrate specificity (23), Cdc48p was shown to be a central component in the retrotranslocation process (24). The mammalian homolog of Cdc48p, AAA-ATPase p97 (p97), has also been implicated in the retrotranslocation of various ERAD substrates (25). Release of target proteins into the cytosol appears to involve binding to p97, and an ATP-dependent change in p97 conformation, which then drives polypeptide retrotranslocation (26). Observations in cultured cells demonstrating apoB polyubiquitination (5) have suggested that apoB may be a potential substrate for p97-mediated retrotranslocation. In this study, we have investigated the potential role of the AAA-ATPase p97 in the proteasomal degradation of apoB in HepG2 cells.

MATERIALS AND METHODS

Cell culture

HepG2 cells were obtained from the American Type Culture Collection (Manassis, VA; HB-8065). Cells were maintained in 10 cm culture dishes (Falcon) in DMEM (Invitrogen Corp., Burlington, ON) containing 10% (v/v) FBS and 2 mM glutamine. Cells were split at approximately 70–80% confluence, every 2 days, by trypsinization and replating at a ratio of 1:3. More-dilute replating resulted in cells that would no longer grow in monolayer and could therefore not be used for experiments, particularly those involving digitonin permeabilization. For most of the experiments, the cells were plated onto 35 mm Primaria dishes, whereas for small interfering ribonucleic acid (siRNA) transfections the cells were plated onto standard 12-well tissue culture plates. Cells were maintained in a 37°C humidified incubator with 5% CO_2 atmosphere. Where indicated, 70–80% confluent monolayers were treated with MG132 (BIOMOL International, Plymouth Meeting, PA) (25 μM from a DMSO stock solution), tunicamycin (5 μg/ml in DMSO), or DTT (2 mM in water) for the specified time interval, as described in the figure legends.

Metabolic labeling

HepG2 cells, in 35 mm Primaria dishes at approximately 70–80% confluence, were incubated in cysteine/methionine-free DMEM for 1 h and then labeled for up to 60 min in the same medium containing 100 μCi of [^{35}S]cysteine/methionine (Express Protein Labeling Mix; Perkin-Elmer, Boston, MA), in the absence or presence of 25 μM MG132 (BIOMOL International). For measurement of initial rates of synthesis, the labeling medium was removed at the indicated time and the cells were recovered by lysis in a radioimmunoprecipitation assay (RIPA) buffer (50 mM Tris-HCl, pH 8.0, 150 mM NaCl, 1 mM EDTA, 1% Triton X-100, 1% sodium deoxycholate) containing 1% SDS as previously described (27). For pulse-chase analysis of apoB stability and secretion, the labeling medium was removed after a 1 h pulse and the monolayers were incubated with DMEM containing 10 mM methionine and 0.6 mM cysteine. Cells and medium were collected, after chase incubation for up to 4 h, by lysis as described above.

Immunoprecipitation

Cell and medium samples were adjusted to 0.1% SDS, and apoB protein was collected by immunoprecipitation with a goat polyclonal antibody to human apoB (AB742; Chemicon International, Inc., Temecula, CA). Where indicated, nonimmune goat serum was used in control immunoprecipitations. Immunocomplexes were recovered on protein A Sepharose beads (Amersham Biosciences, Inc.; Baie d'Urfé, Quebec, Canada), washed extensively, and eluted into SDS-PAGE sample buffer. ApoB-100 was resolved by SDS-PAGE (5%) and visualized by autoradiography. Bands were excised, and radioactivity was quantified by liquid scintillation counting. Similarly, polyclonal antibody to human apoA-I (Roche Diagnostics; Laval, Quebec, Canada) was used to immunoprecipitate HepG2 apoA-I, and immune complexes were resolved by SDS-PAGE on 10% (w/v) polyacrylamide gels.

Digitonin permeabilization of HepG2 Cells

Confluent monolayers of HepG2 cells in 60 mm dishes were incubated with 1 ml of CSK buffer (10 mM PIPES, pH 6.8, 0.3 M sucrose, 0.1 M KCl, 2.5 mM $MgCl_2$, 1 mM sodium-free EDTA) with or without 75 μg/ml of digitonin for 10 min on ice (28). Cell and cytosol fractions were collected and solubilized in 1% SDS as described above.

Immunoblotting

Proteins were resolved by SDS-PAGE, transferred to nitrocellulose membranes, and visualized by immunoblotting with antibodies to apoB (1D1; Ottawa Heart Institute Research Corp.; Ottawa, Ontario, Canada), apoA-I (5F6, Ottawa Heart Institute Research Corp.), calnexin (SPA-860, Stressgen Bioreagents, Ann Arbor, MI), protein disulfide isomerase (PDI) (SPA-891; Stressgen), p97 (PRO65278; Research Diagnostics Inc., Concord, MA), heat shock protein 70 (SPA-820; Stressgen), GRP78 (GL-19, Sigma-Aldrich), actin (MAB1501, Chemicon), or the β1 subunit of the 20S proteasome (PW8140; BIOMOL Int.). Secondary antibodies were mouse- or rabbit-specific HRP conjugates, purchased from Chemicon. All immunoblots were developed using BM chemiluminescence (POD) from Roche Diagnostics.

Preparation of HepG2 cytosol

Confluent HepG2 cells, in 10 cm dishes, were gently scraped into microsome buffer (10 mM Tris-HCl, pH 7.4, 250 mM sucrose) and passed 20 times through a ball-bearing homogenizer. Nuclei were pelleted by centrifugation at 4°C for 10 min at 9,500 rpm in an SS34 rotor (Sorvall Instruments), and organelles were removed from the postnuclear supernatant fraction by centrifugation at 4°C for 18 min at 100,000 rpm in a TLA100.4 rotor (Beckman-Coulter; Mississauga, Ontario, Canada). The supernatant cytosol was collected and used for reconstitution experiments. An ATP-generating cocktail (1 mM ATP, 5 mM $MgCl_2$, 5 mM creatine phosphate, 100 μg/ml creatine kinase) was added in cytosol reconstitution experiments.

Ubiquitination analysis

HepG2 cells were incubated in the absence or presence of 25 μM MG132 or 100 μM ALLN (Roche Diagnostics) for 1 h. Cells were then permeabilized with 75 μg/ml digitonin for 10 min on ice, and cytosol and cell fractions were collected. After addition of 0.1% SDS, apoB was collected by immunoprecipitation with polyclonal antibody to human apoB and protein A Sepharose, as described above. After extensive washing in RIPA buffer containing 0.1% SDS, the immunoprecipitant apoB was resolved by SDS-PAGE (5%), transferred to nitrocellulose, and immunoblotted with monoclonal antibodies to apoB (1D1) or ubiquitin (SPA-203; Stressgen).

Chemical cross-linking and nondenaturing immunoprecipitation

For chemical cross-linking, confluent HepG2 cells, grown in 10 cm dishes, were gently scraped into PBS (41 mM Na_2HPO_4, 4 mM KH_2PO_4, 138 mM NaCl, 2.5 mM KCl). Dithiobis(succinimidylpropionate) (DSP; Pierce Biotechnology, Inc., Rockford, IL) was added from a 500 mM stock solution (in DMSO) to a final concentration of 2.5 mM and incubated for 30 min at 37°C. Excess DSP was inactivated by incubation for 15 min in the presence of 50 mM Tris-HCl, and cells were lysed in RIPA buffer containing 1% SDS. Samples were diluted to 0.1% SDS, and cross-linked apoB complexes were recovered by immunoprecipitation with goat antibody to human apoB or, to control for nonspecific interactions, with nonimmune goat serum. Immunocomplexes were collected on protein A Sepharose, washed extensively, and eluted into 2% SDS sample buffer with reducing agent (100 mM DTT). Proteins were resolved by SDS-PAGE (5%), transferred to nitrocellulose membranes, and visualized by blotting with antibodies to apoB and p97, as described above.

Nondenaturing immunoprecipitations were also performed to demonstrate the interaction between apoB and p97. Near-confluent (70–80%) monolayers of HepG2 cells were treated with or without 25 μM MG132 for 1 h and washed twice with PBS. Cells were lysed for 1 h at 4°C in 50 mM Tris-HCl, pH 8.0, 50 mM NaCl, 5 mM EDTA, 20% sucrose, 1% Nonidet P40 (Roche Diagnostics) with Complete® (Roche Diagnostics) protease inhibitor cocktail. Immunoprecipitates were then collected overnight with nonimmune serum or antibodies to apoA-I or apoB in the presence of protein A Sepharose. After washing extensively with lysis buffer, the immunocomplexes were released into SDS-PAGE sample buffer and analyzed as described above.

Reduction of HepG2 p97 with siRNA

For each well of a 12-well plate, a transfection medium was prepared containing either nontargeting siRNA #1 (Dharmacon, Inc.) or p97/VCP siRNA ID:119276 (si-p97, Ambion, Inc., Austin, TX) and 1.5 μl siPORT *NeoFX* transfection reagent (Ambion, Inc.) adjusted to a final volume of 100 μl using Opti-MEM I media (Invitrogen). HepG2 cells at 70–80% confluence were trypsinized and resuspended in low-serum growth medium (2% FBS in DMEM). Cell suspension was added to the 100 μl transfection medium in each well to a final volume of 1 ml and siRNA concentration of 30 nM. The transfection medium was removed and replaced with growth medium after 24 h, and subsequent analyses were performed 72 h following transfection. The effectiveness of the siRNA was assessed by immunoblotting of cell lysates for p97 and semiquantified by densitometric analysis of the immunoblots using Scion Image© (Scion Corporation, Frederick, MD).

Sucrose density ultracentrifugation

Growth medium was removed from confluent HepG2 cells in 60 mm dishes and replaced with serum-free DMEM for 2 h. Medium was collected, and cytosol was prepared by digitonin permeabilization of HepG2 cells treated with 25 μM MG132 for 1 h. Medium and cytosol were brought to 12.5% sucrose, and a discontinuous sucrose gradient was prepared as described previously (29). After ultracentrifugation for 20 h at 55,000 rpm in a SW60Ti rotor, 13 fractions of 330 μl were collected. Proteins were concentrated by TCA precipitation, solubilized in SDS-PAGE sample buffer, and resolved by 5% SDS-PAGE. ApoB and Hsp70 proteins were detected by immunoblotting.

RESULTS

Intracellular degradation of apoB-100 is markedly reduced in permeabilized HepG2 cells

To evaluate the role of cytosolic components in apoB degradation, we compared the effect of MG132 and digitonin permeabilization on the stability of intracellular apoB. In pulse-chase experiments (**Fig. 1A**, **B**, Intact), apoB-100 radiolabel was degraded with a half-life of approximately 2 h. When the proteasome inhibitor MG132 (25 μM) was included in the chase medium, apoB-100 half-life was extended to approximately 4 h (Fig. 1A, B, Intact/MG132), although most of the effect of MG132 was evident only during the first hour of chase. In contrast, permeabilization of the HepG2 cells following the pulse essentially abolished the posttranslational degradation of apoB-100 (Fig. 1A, B, Permeabilized). Less than 10% of the initial apoB-100 was secreted from intact cells, and this was unaffected by MG132 treatment (data not shown). These results are consistent with the role of the cytosolic proteasome in the early posttranslational degradation of apoB-100 in the HepG2 cell. Indeed, degradation could be partially reconstituted by the addition of freshly prepared HepG2 cytosol (0.7 mg/ml in DMEM) and an ATP generating system (17) to the permeabilized cells (Fig. 1C). Nevertheless, nonproteasomal mechanisms of degradation are also involved, inasmuch as proteasome inhibition with MG132 was not sufficient to reduce apoB-100 degradation beyond 1 h of chase.

Distribution of proteins involved in ERAD

We then examined the distribution of known ERAD factors in the membranes and cytosol of HepG2 cells, to identify candidate proteins that may be involved in the retrotranslocation and delivery of apoB to the cytosol for deg-

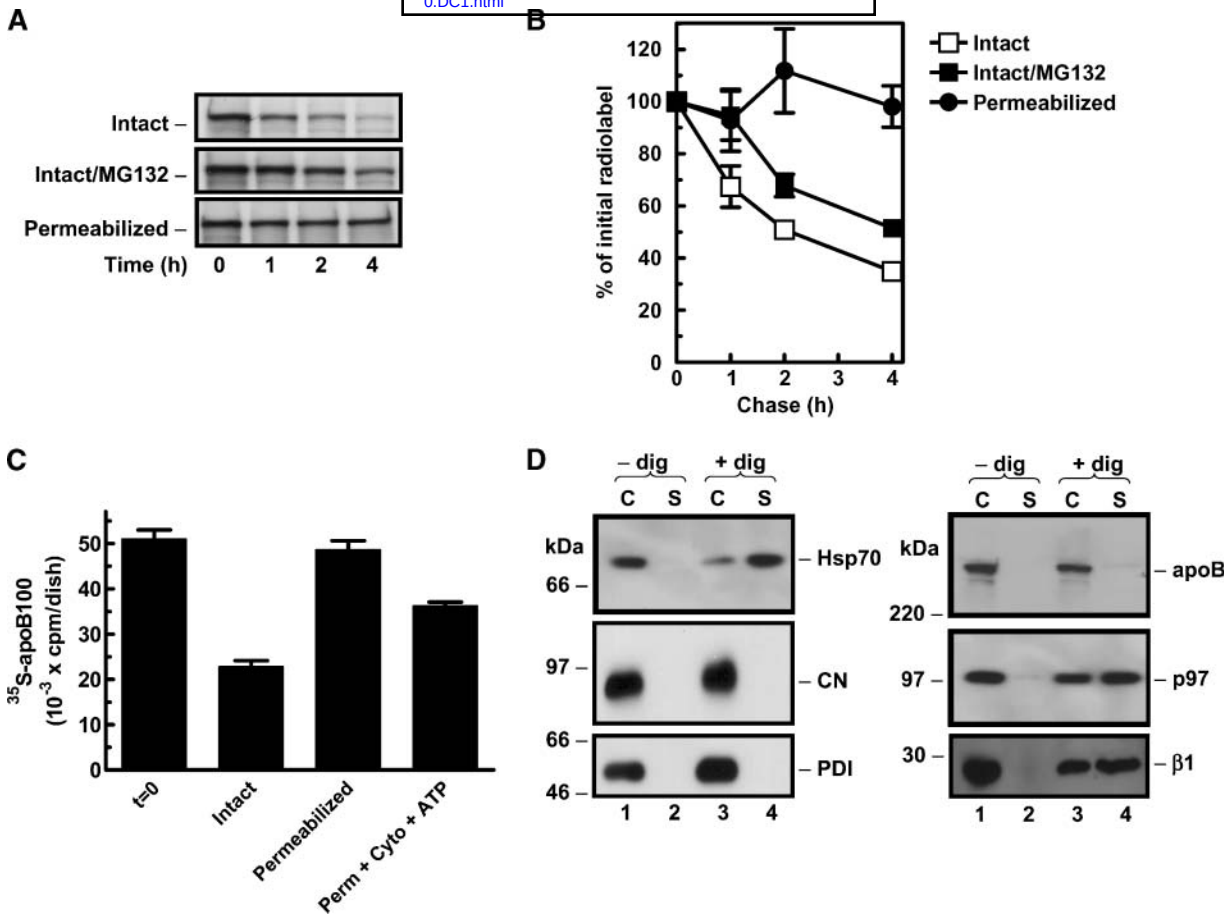

Fig. 1. Permeabilization of HepG2 cells markedly decreases the degradation of apolipoprotein B-100 (apoB-100). HepG2 monolayers were pretreated for 1 h with or without the proteasome inhibitor MG132 (25 μM) and pulse-labeled for 1 h with [35S]methionine/cysteine (200 μCi/ml). After labeling, one set of dishes was permeabilized with digitonin, whereas the remaining dishes were left intact. The supernatant was removed and replaced with medium with or without MG132 for chase of up to 4 h. At each time point, cells were collected by lysis into 1% SDS-radioimmunoprecipitation assay buffer, and apoB-100 was immunoprecipitated and visualized by SDS-PAGE with autoradiography. A: Autoradiographs of digitonin-permeabilized cells (Permeabilized) and intact cells treated with (Intact/MG132) or without (Intact) proteasome inhibitor. B: Radioactivity in apoB-100 was determined by liquid scintillation counting of the excised band, expressed as percent of the radiolabel at the initiation of the chase. Data points represent the mean ± SD of three independent experiments. Open square, intact; closed square, intact/MG132; closed circle, permeabilized. C: Replicate dishes of HepG2 cells were pulse-labeled as described above. During the 2 h chase, intact or permeabilized cells were incubated with DMEM or DMEM containing HepG2 cytosol (0.7 mg/ml) and an ATP-generating cocktail (1 mM ATP, 5 mM creatine phosphate, 5 mM $MgCl_2$, and 100 μg/ml creatine kinase). ApoB-100 radioactivity was determined as described for B. Each bar represents the mean ± SD (n = 3). D: Western blot analysis of cell (C) and supernatant (S, cytosol) fractions of HepG2 cells following digitonin permeabilization. Cells were treated with or without digitonin, and the cell and supernatant fractions were collected. Aliquots of cell and supernatant protein were resolved by 3–15% gradient SDS-PAGE and transferred to nitrocellulose. Membranes were incubated with the indicated antibody and visualized by enhanced chemiluminescence. dig, digitonin; p97, AAA-ATPase p97; β1, 20S proteasome β1 subunit; Hsp70, cytosolic heat shock protein 70 kDa; CN, calnexin; PDI, protein disulfide isomerase.

radation. When HepG2 cells were permeabilized with digitonin, essentially all of the cytosolic Hsp70 was released (Fig. 1D), whereas the ER-resident PDI and calnexin remained associated with the cell membranes. Similarly, apoB-100 was found almost exclusively with the cell membrane fraction, although a small amount of apoB-100 could be detected in the cytosol in longer exposures. In contrast, we found that the AAA-ATPase p97 (p97) and components of the 20S subunit of the proteasome (β1, Fig. 1D and β4, not shown) were equally distributed in the cell and cytosol fractions. Although high-salt washing was able to remove a portion of p97 and proteasomal proteins from the membranes (data not shown), these components seemed to be tightly associated with the cell membrane system, perhaps at the outer leaflet of the ER membrane. Because an interaction between p97 and other ERAD substrates has been implicated in retrotranslocation to the cytosol (24), we examined this possibility for apoB-100 using cross-linking and nondenaturing immunoprecipitation.

Intracellular apoB-100 is in complex with AAA-ATPase p97

Potential interacting partners of apoB-100 were captured using a membrane-permeable, thiol-cleavable cross-linking agent, DSP. When intact HepG2 cells were incubated with DSP, p97 was found in complex with apoB by immunoprecipitation. ApoB immunoprecipitates from cells treated with DSP were resolved on reducing gels (**Fig. 2A**) and contained both apoB-100 (lane 4) and p97 (lane 8). We

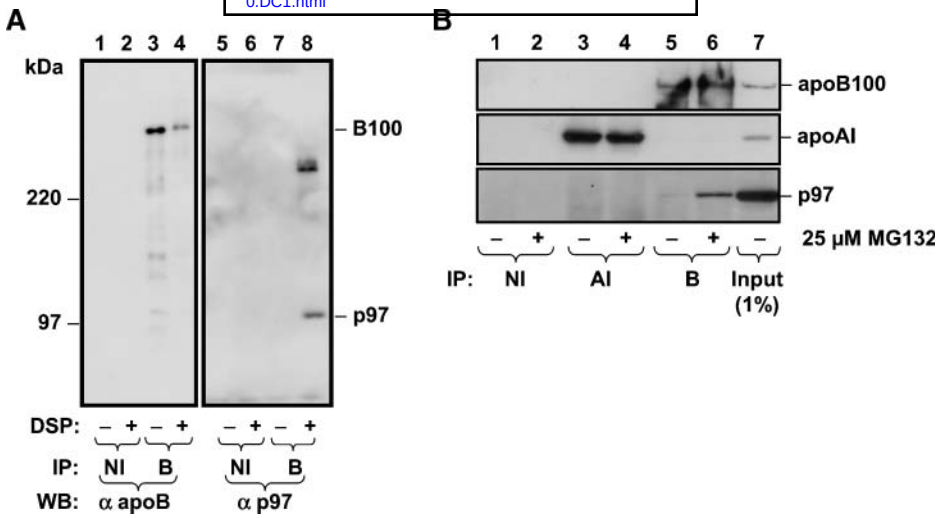

Fig. 2. AAA-ATPase p97 is associated with apoB-100 in intact HepG2 cells. A: HepG2 cells were incubated with or without 2.5 mM of the membrane-permeable, thiol-cleavable cross-linking agent, dithiobis(sulfosuccinimidylpropionate) (DSP), for 1 h at room temperature. Tris-HCl, pH 7.4, was added to 50 mM, and the incubation was continued for an additional 15 min. The cells were then lysed in 1% SDS buffer and subjected to immunoprecipitation (IP) with polyclonal anti-apoB serum (B) or with nonimmune serum (NI). Immunocomplexes were then released into reducing (100 mM DTT) sample buffer and separated on 5% SDS-PAGE gels. Resolved proteins were transferred to nitrocellulose and visualized using monoclonal antibodies to apoB (left panel) or p97 (right panel) with chemiluminescence detection. B: HepG2 cells were incubated with or without 25 μM MG132 for 1 h and then lysed with 1% Nonidet P40. Lysates were cleared by centrifugation, and aliquots were subjected to immunoprecipitation with nonimmune serum (NI), anti-apoA-I (AI), or anti-apoB (B) antiserum. Immunoprecipitates or input lysate were resolved by SDS-PAGE, transferred to nitrocellulose, and visualized by immunoblotting with the indicated antibodies and chemiluminescence detection.

observed p97 as both a monomer and a higher-molecular-weight form (~300 kDa) despite the reducing conditions. Neither apoB nor p97 was found in immunocomplexes prepared using nonimmune serum (lanes 1, 2, 5, and 6). In addition, nondenaturing immunoprecipitation (Fig. 2B) was able to capture p97 in association with apoB (lanes 5 and 6) but not with apoA-I (lanes 3 and 4). The interaction with apoB was also increased with proteasome inhibition (compare lane 6 to lane 5). These studies suggested that apoB may be a substrate for p97-mediated retrotranslocation.

Ubiquitinated apoB accumulates in the cytosol of MG132-treated HepG2 cells

We next sought to dissociate proteasomal degradation from retrotranslocation of apoB-100 as a first step toward the identification of cytosolic components involved in apoB retrotranslocation. HepG2 cells were treated with MG132 (25 μM) to inhibit proteasomal proteolysis, and ubiquitinated apoB-100 in the cytosol and organelle-associated fraction (i.e., that remaining with the monolayer following permeabilization) were recovered by immunoprecipitation and visualized by immunoblotting. To visualize cell and cytosol fractions on the same blots, all of the cytosol and approximately 10% of the cell lysate were loaded onto the gel. A small amount of cytosolic apoB-100 could be detected in cells without MG132 treatment (**Fig. 3A**, lane 7), and treatment with MG132 increased cytosolic apoB-100 (Fig. 3A, lane 8). We estimate that the amount of apoB-100 in the cytosolic fraction is ~1% of the total cellular apoB without MG132 and perhaps as high as ~5% of cellular apoB in the presence of MG132. We observed a similar increase in cytosolic apoB-100 when cells were treated with 100 μM ALLN (data not shown). This is consistent with the observations of Liao and colleagues (30). Cytosolic and organelle-associated apoB were both polyubiquitinated in MG132-treated cells (Fig. 3B, lanes 8 and 6, respectively), but polyubiquitinated species were not detectable in cells without MG132 because of the very active proteasomal degradation of apoB-100 in HepG2 cells (Fig. 3B, lanes 5 and 7). Most of the polyubiquitinated apoB species in MG132-treated cells were in the cytosol, even though this is a much smaller portion of the total apoB. Polyubiquitinated species of various sizes were observed as a smear on the gel because of the presence of partial apoB chains, possibly representing cotranslational degradation products (4, 18). Control immunoprecipitations were used to rule out the possibility that the ubiquitin-reactive material could be due to nonspecific precipitation of unrelated ubiquitinated proteins (Fig. 3A, B, lanes 1 to 4). The presence of full-length apoB-100 in the cytosol suggested that in the absence of proteolysis by the proteasome, some apoB can be extracted from the endomembrane system into the cytosol.

To assess the lipid content of cytosolic apoB, we characterized the secreted and cytosolic apoB proteins by density gradient ultracentrifugation (see supplementary Fig. I). Secreted apoB from HepG2 cells was found primarily in the LDL fractions of the gradient, as shown previously (31). Cytosolic apoB-100 was found only near the bottom

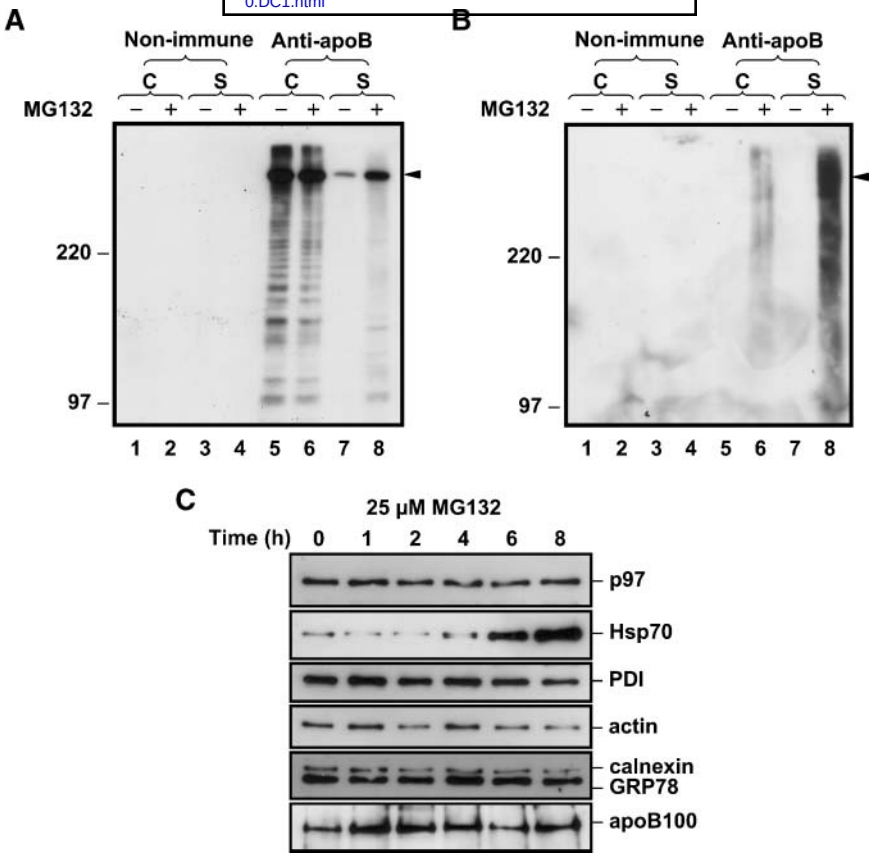

Fig. 3. Ubiquitinated apoB-100 accumulates in the cytosol of cells treated with MG132. A: HepG2 cells were incubated with or without MG132 (25 μM) for 1 h, and the monolayers were then permeabilized with digitonin as described in Materials and Methods. The resulting permeabilized cell (C) and supernatant (S, cytosol) fractions were collected, and immunoprecipitates were prepared with either polyclonal anti-apoB or nonimmune goat serum. Aliquots of each immunocomplex were resolved by 5% SDS-PAGE, and following transfer of the proteins to nitrocellulose, human apoB was revealed by Western blot analysis. Arrowhead indicates the mobility of full-length apoB-100. B: Aliquots of immunoprecipitates prepared as in A were visualized with monoclonal anti-ubiquitin antibody. C: HepG2 monolayers were treated with 25 μM MG132 for up to 8 h, and cells were collected by lysis. Equal amounts of total cell protein were fractionated on SDS-PAGE gels and probed for the indicated protein. GRP78, glucose-regulated protein 78 kDa.

of the density gradient, in fractions that also contain proteins associated with little or no lipid, such as Hsp70. This observation suggested that cytosolic apoB is lipid-poor, lipid-free, or associated with other proteins that increase its density by decreasing the lipid:protein ratio.

To explore the changes in the expression of ERAD-associated proteins caused by proteasome inhibition, we used a time course of MG132 treatment and monitored the levels of proteins of the unfolded protein response (UPR) and cytosolic heat shock response. HepG2 cells were incubated with 25 μM MG132 for up to 8 h, and proteins were revealed by Western blotting (Fig. 3C). Substantial accumulation of apoB-100 was observed after 1–2 h, and large increases in Hsp70 were observed after 6–8 h. No changes in p97, actin, calnexin, or PDI were observed during the 8 h experiment, whereas GRP78 increased modestly, beginning at about 4 h. Thus, the most-profound changes were in the cytosolic stress marker protein, and this is consistent with previous observations in this cell model (32). However, after 1 h, there were no profound changes in any protein except apoB, suggesting that apoB accumulation was the result of a block in its normal rate of turnover, rather than a generalized stress response to the MG132.

Reduction of cellular p97 increases cellular apoB-100

If p97 is necessary, or is part of a complex that is necessary, for retrotranslocation of apoB, a reduction of HepG2 p97 would be expected to impair the retrotranslocation process and decrease proteasomal degradation of apoB-100. A knockdown approach was used to reduce the level of p97, using double-stranded siRNA targeting the p97 transcript. HepG2 cells were transfected with nontargeting siRNA or siRNA targeting p97 (si-p97), each at a concentration of 30 nM. As shown in **Fig. 4A**, 72 h after transfection, there was a decrease in cellular p97 in cells transfected with the targeting siRNA (24 ± 9% of mock, n = 8) but not in cells transfected with the nontargeting siRNA (99 ± 16% of mock, n = 6). In contrast to the observations in cells treated with MG132 (Fig. 3C), there were no increases in Hsp70 with p97 knockdown (Fig. 4A), and PDI and calnexin were also unaffected. In fact, the levels of Hsp70 were decreased, compared with the nontargeting siRNA. GRP78

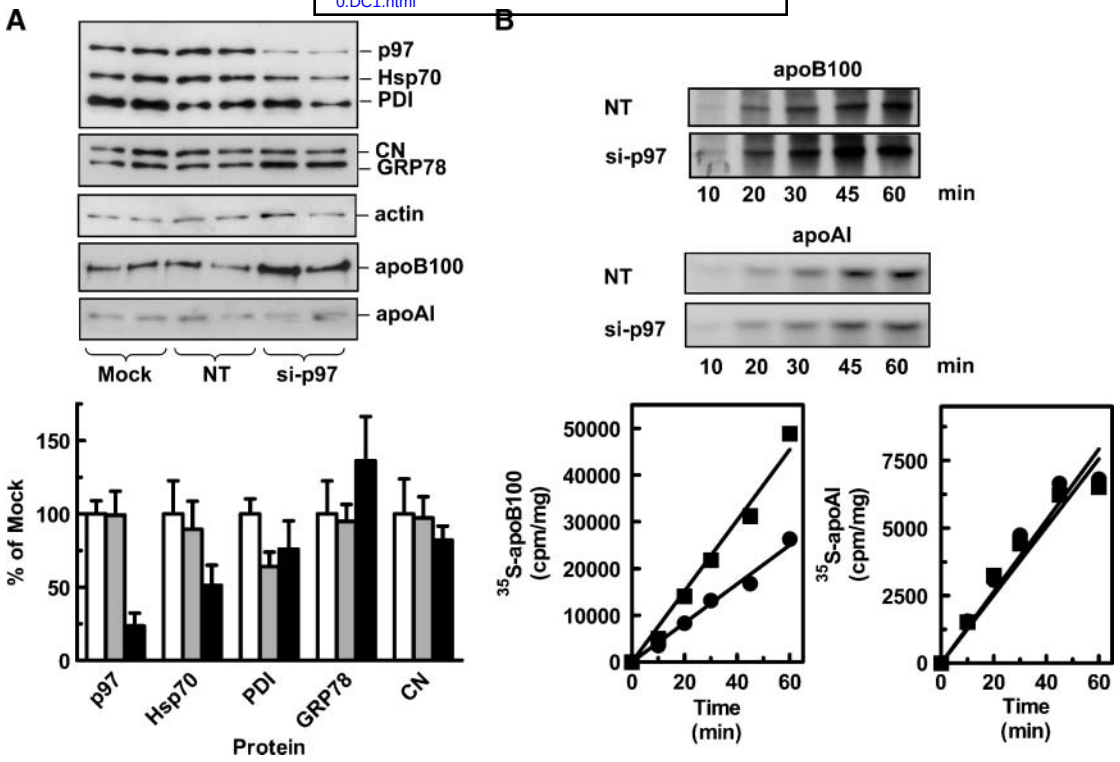

Fig. 4. Small interfering ribonucleic acid (siRNA)-mediated reduction of cellular p97 increases HepG2 apoB-100. A: Monolayers of HepG2 cells were transfected with nontargeting (NT, gray bars), p97-targeted siRNA (si-p97, black bars), or mock-transfected (Mock, white bars). Seventy-two hours posttransfection, cells were collected, and p97 and proteins indicated were visualized by Western blot analysis. Duplicate wells are shown from a representative experiment, repeated three times. Individual proteins were quantified by scanning densitometry and are presented as percentage of the mock-transfected control. Each bar represents mean ± SD (n = 6). B: Biosynthesis of apoB-100 and apoA-I in siRNA-transfected HepG2 cells. Seventy-two hours following transfection with either nontargeting (NT, closed circle) or p97-targeting (si-p97, closed square) siRNA, cells were pulse-labeled with 100 μCi of [35S]methionine/cysteine for up to 60 min. ApoB and apoA-I proteins were immunoprecipitated from cell lysates, resolved by SDS-PAGE, and visualized by autoradiography (top panels). Radioactivity in each protein band was quantified by scintillation counting and normalized for cell protein (lower panels). The figure shows a representative experiment, which was repeated three times. There were no differences in cell protein between the nontargeting and si-p97-treated cells.

was increased by approximately 35%, suggesting that the effects of p97 knockdown modestly affected this luminal chaperone.

To evaluate the effect of reduced levels of p97 on apoB metabolism, transfected HepG2 cells were analyzed by metabolic radiolabeling. In cells transfected with siRNA for p97 (Fig. 4B), accumulation of radiolabeled apoB-100 increased approximately 2-fold, compared with the nontargeting control siRNA, whereas the apoA-I was not affected. These studies suggested that reduction of cellular p97 decreased the turnover of newly synthesized apoB-100.

Pulse-chase experiments were then performed to directly assess the effect of reduced p97 on the posttranslational stability of apoB-100. Compared with nontargeting siRNA, treatment with si-p97 siRNA decreased the posttranslational degradation of apoB-100 during the first hour of chase (**Fig. 5A**) but had no effect on either the stability or the secretion of apoA-I (Fig. 5B). In spite of the decrease in degradation, there was no effect on apoB-100 secretion.

The effects of p97 knockdown on apoB-100 metabolism were not the same as those observed for a UPR resulting from ER stress. The pattern of chaperone protein expression was clearly different with p97 knockdown (Fig. 4A) and MG132 treatment (Fig. 3C). Furthermore, because the levels of apoB increased with p97 knockdown but decreased when ER stress was induced using DTT (see supplementary Fig. 2A) or tunicamycin (see supplementary Fig. 2B), the accumulation of apoB was not likely to have been the result of a classic UPR.

Reduction of cellular p97 reduces cytosolic apoB accumulation and diminishes the protective effect of MG132

To further characterize the role of p97 in apoB degradation, we examined the effect of p97 reduction on the accumulation of polyubiquitinated cytosolic apoB. HepG2 cells were transfected with nontargeting or si-p97 siRNA and permeabilized 72 h thereafter with digitonin. Immunoblotting of cell lysate and cytosolic fractions for calnexin and GRP78 (**Fig. 6A**, lower panel) indicated that the cytosol fractions were free of ER contents. Immunoprecipitation of apoB and immunoblotting showed that MG132 treatment of cells transfected with the nontargeting siRNA caused the expected increase in cell-associated (Fig. 6A, lane 2 vs. lane 1) and cytosolic apoB-100 (Fig. 6A, lane 4 vs. lane 3). In contrast, the cells transfected with si-p97 siRNA were resistant to the effects of MG132 on apoB-100 levels

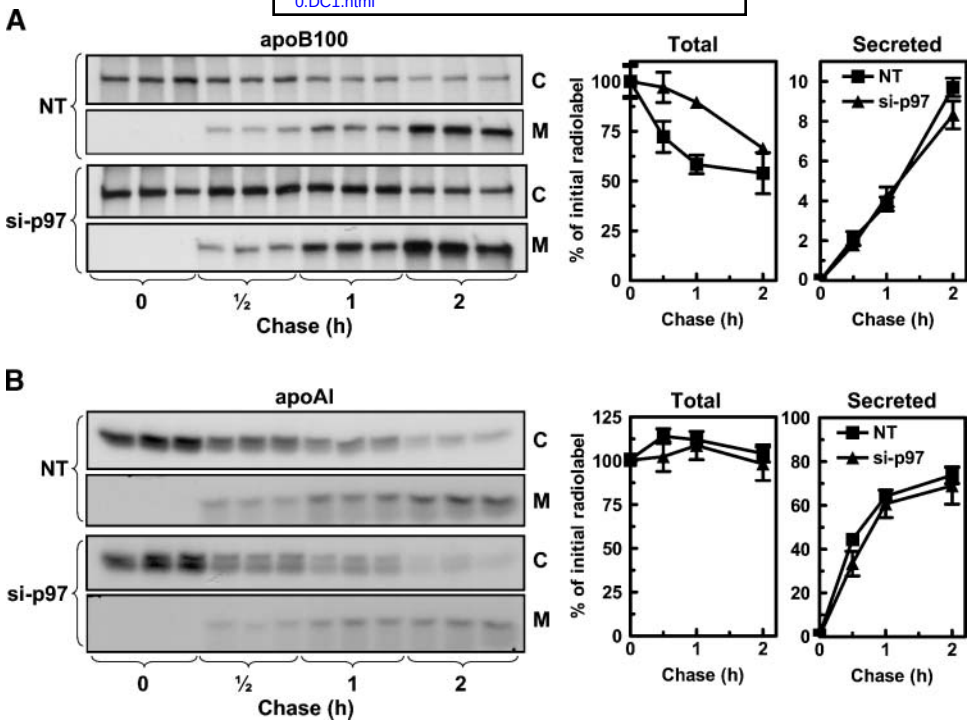

Fig. 5. siRNA-mediated reduction of cellular p97 increases HepG2 apoB-100 stability but not its secretion efficiency. Autoradiographs and quantitation of apoB-100 (A) or apoA-I (B) in cells (C) and medium (M) by pulse-chase analysis. Seventy-two hours following transfection, HepG2 monolayers were labeled with [35S] methionine/cysteine for 1 h and then chased for up to 2 h as described in Materials and Methods. At each time point, apoB or apoA-I was recovered from cells and medium by immunoprecipitation and visualized by autoradiography. Cellular decay (Total = cells plus medium) and secretion of apolipoprotein radioactivity are expressed as percent of initial radiolabel. Autoradiographs and curves depict triplicate wells from a representative experiment that was repeated three times. Error bars represent ± SD.

in the lysate (Fig. 6A, lane 6 vs. lane 5) and in the cytosol (Fig. 6A, lane 8 vs. lane 7). Cell lysate apoB-100 mass was not markedly increased after reduction of p97 (Fig. 6A), even though newly synthesized apoB-100 was increased (Fig. 4B); in some immunoblotting experiments, apoB-100 mass increases were evident (Fig. 4A and data not shown). Nevertheless, treatment with si-p97 siRNA consistently prevented the accumulation of polyubiquitinated apoB species in the cytosol with MG132 treatment (Fig. 6B, lane 8 vs. lane 4), reflecting the decrease in cytosolic apoB-100. However, polyubiquitinated apoB species were detectable in the cell lysate fractions of si-p97 cells with MG132 treatment (Fig. 6B, lane 2 vs. lane 6). Taken together, these results suggest that p97 knockdown and MG132 treatment affect the same degradation pathway and that p97 is required for the movement of apoB from the organelle fraction into the cytosol for proteasomal degradation.

DISCUSSION

The present work has evaluated the role of p97 in the delivery of apoB-100 to the cytosolic proteasome for degradation. Digitonin permeabilization of HepG2 cells indicated that degradation of newly synthesized apoB-100 was minimal if cytosolic components were removed, an observation that confirms a previous report (33). This suggests that cytosolic proteasomal proteolysis is the dominant form of apoB degradation in this cell line. ApoB-100 degradation was partially reconstituted by adding back HepG2 cytosol, indicating that cytosolic components are central to this degradation, even though some elements of the degradation pathway (p97, proteasome core components) remain associated with the cellular membrane fraction. Nevertheless, digitonin-permeabilized HepG2 cells have been shown to have additional posttranslational degradation pathways, such as the lumenal ER protease, ER-60 (6).

In this study, we have shown that two steps involved in apoB ERAD, retrotranslocation and degradation, can be uncoupled. Inhibitors of the proteolytic activity of the 20S subunit of the proteasome have been used to demonstrate the accumulation of other ERAD substrates in the cytosol (34–37), suggesting that for many substrates, the proteolytic activities of the proteasome and retrotranslocation are separable. Similarly, proteasome inhibition in HepG2 cells resulted in the accumulation of polyubiquitinated apoB proteins in the cytosol. This finding extends previous observations of cytosolic apoB demonstrated biochemically (30) and by immunofluorescence microscopy (38, 39). However, experiments with agents that inhibit the proteolytic activity of β-subunits of the 20S proteasome do not exclude the possibility that activities of the 19S subunit may be involved in the retrotranslocation of ERAD substrates. Mitchell et al. (40) reported that retrotranslocation and

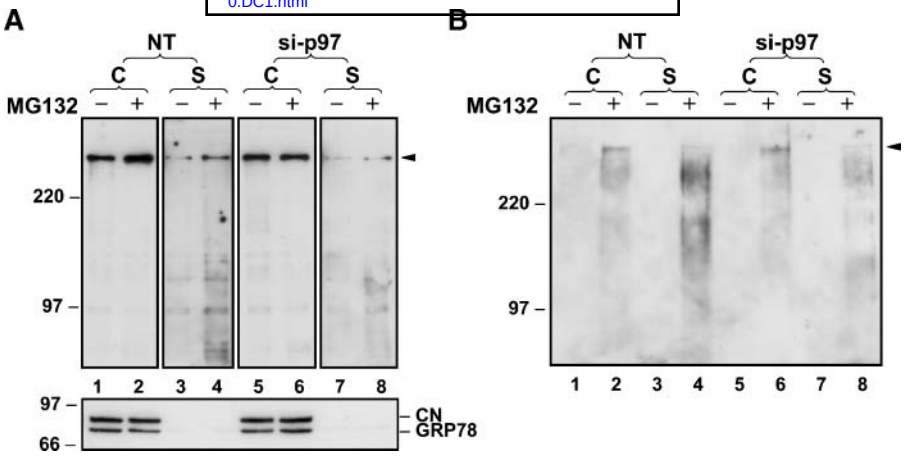

Fig. 6. siRNA-mediated reduction of cellular p97 affects apoB proteasomal degradation by decreasing the release of apoB into the cytosol. A: Western blot analysis of cytosolic apoB-100 after siRNA transfection. HepG2 cells were transfected with nontargeting (lanes 1–4) or p97-targeting siRNAs (lanes 5–8). Seventy-two hours following transfection, cells were incubated with MG132 (25 μM) for 1 h, permeabilized with digitonin, and cellular (C) and cytosolic (S) proteins were collected. Immunoprecipitates were prepared with polyclonal anti-apoB serum. Equal amounts of each immunocomplex were resolved by 5% SDS-PAGE, and following transfer of the proteins to nitrocellulose, human apoB was revealed by Western blot analysis. Cellular panels are 1 s exposures, cytosol panels are 60 s exposures of the same membrane. Arrowhead indicates the mobility of full-length apoB-100. In the lower panel, equivalent volumes of cellular and cytosolic proteins were resolved by 10% SDS-PAGE and probed for calnexin (CN) and GRP78 by Western blot analysis. B: Aliquots of immunoprecipitates prepared as in A were visualized with monoclonal anti-ubiquitin antibody. The figure shows a representative experiment that was repeated three times.

proteasomal degradation of apoB in HepG2 cells are tightly coupled and that apoB does not accumulate to any extent in the cytosol. A recent in vitro study of the cystic fibrosis transmembrane-conductance regulator degradation has suggested that the accumulation of full-length ERAD substrates in the cytosol during proteasome inhibition may be the result of the uncoupling of peptidase activities of the 20S core from the unfolding and delivery by ATPase activities of the 19S subunit (37) as established in the yeast ERAD system (41). Our studies with p97 knockdown and proteasome inhibition suggest that apoB-100 is an ERAD substrate for which retrotranslocation and proteasome-mediated degradation can be dissociated.

The present work has provided additional evidence for the role of the AAA-ATPase p97 in the retrotranslocation of ERAD substrates (as reviewed in Refs. 25, 42). The presence of p97 in association with the endomembrane system after permeabilization is consistent with the existence of a retrotranslocation complex containing p97 on the ER membrane (43). Cross-linking and nondenaturing immunoprecipitation demonstrated that p97 was in association with apoB-100, suggesting that p97 may be involved in recognition of apoB for ERAD. In addition, reducing the level of p97 in HepG2 cells decreased apoB-100 turnover and reduced its accumulation in the cytosol, suggesting that p97 is involved in one step that is necessary for proteasomal degradation of apoB-100.

p97-mediated retrotranslocation has been suggested to require the polyubiquitination of ERAD substrates (44), and for apoB, this probably occurs while the protein is partially in the ER and spanning the translocation channel. Because the majority of the polyubiquitinated species that accumulate in the presence of MG132 are found in the cytosol (Fig. 3B) and are associated with the full-length apoB-100, our results suggest that apoB becomes polyubquitinated as, or immediately before, it is released into the cytosol. Thus, we suggest that polyubiquitination precedes and may signal the release of apoB-100 into the cytosol. Although our study has examined primarily the full-length apoB-100, the presence of a spectrum of polyubiquitinated apoB proteins in the cytosol is consistent with cotranslational polyubiquitination of apoB-100 in HepG2 cells (45) and suggests that targets for p97-mediated retrotranslocation may include partially translated apoB-100 polypeptides. By reducing the level of p97 or by treating the cells with MG132, we decreased apoB-100 turnover and enhanced the early posttranslational stability of the full-length protein. However, the stabilization of apoB, in itself, did not enhance apoB secretion. Lipid availability is likely to be more important in determining the level of apoB-100 secretion (46), inasmuch as even those apoB proteins that escape ERAD can be degraded by other mechanisms.

Knockdown of p97 to 25% of control level in HepG2 cells did not elicit a profound UPR. Ota, Gayet, and Ginsberg (47) recently demonstrated that apoB secretion is compromised by moderate ER stress levels in response to fatty acids. Our observation that apoB-100 secretion is unchanged following p97 knockdown suggests that this experiment did not cause sufficient ER stress to affect cell function globally. This is further supported by the lack of an effect on apoA-I metabolism. Tunicamycin and DTT, both known to cause ER stress, reduced HepG2 apoB levels, whereas p97 knockdown decreased apoB-100 turnover and increased cellular apoB-100 mass. The lack of ER stress could

be because a portion of functional p97 remains, under the conditions of our siRNA experiment, retaining some protection against ER dysfunction. In HeLa cells (48), reduction of p97 by more than 85% with RNA interference caused an ER stress response and swelling of the organelle. In Rat-1 fibroblasts, 62% reduction in p97 was insufficient to cause the accumulation of polyubiquitinated proteins, but did have a specific effect on the ubiquitination and half-life of the inositol-1,4,5-trisphosphate receptor, a known endogenous ERAD substrate (49). The discrepancies between studies may be related to cell type or level of p97 reduction. Given the abundance of p97 and its multiple cellular functions, specific cell types may have different requirements. The reason for the absence of a substantial stress response in our system is not clear, although because HepG2 cells secrete many proteins, they may have an inherently high protein folding capacity and could be relatively resistant to the increased burden of misfolded ERAD substrates caused by reductions in p97. Therefore, the siRNA knockdown of p97 seems to affect apoB-100 metabolism, even though a generalized stress response is not observed.

In light of our findings, we propose that the proteasomal degradation of apoB-100 occurs in a manner similar to that seen in other ERAD substrates. When translocation of apoB is arrested and the polypeptide is exposed to the cytosol, the bitopic topology is comparable to that of other ERAD substrates that are membrane integrated (50). p97 may initiate ERAD by interaction with polyubiquitinated apoB, inasmuch as it is generated by the E3 ligase gp78 (18), because it has been suggested that gp78 and p97 and may couple polyubiquitination to retrotranslocation for other substrates (51). Recently, it has been shown that Ufd1 binding to gp78 or p97 is a mutually exclusive event and that binding of polyubiquitin chains of substrate proteins by Ufd1 is critical for ERAD (52). The p97-mediated retrotranslocation of polyubiquitinated apoB may also be guided by Hsp70 and Hsp90, chaperones that have been suggested to facilitate the delivery of polyubiquitinated targets to the 19S subunit of the proteasome (17). During retrotranslocation, continuous delivery of apoB to the 20S core may require the combined ATPase activities of both p97 and proteins in the 19S lid. Hence, the proximity of p97 and the 26S proteasome at the site of apoB-100 translocation may explain how apoB-100 is rapidly directed for cotranslational degradation (40, 45). More work is required to examine the details and sequence of these events.

Cytosolic apoB-100 was found in the HDL range, a density similar to that of LpBs found in the lumen of the ER in digitonin-permeabilized HepG2 cells (53). Because the initiation of lipoprotein assembly begins during the translation of apoB, it is conceivable that disassembly of the lipid-protein complex must occur to allow the polypeptide to transit back through the translocation channel toward the cytosol. The density of the apoB-100 in the cytosol fraction, apparently associated with little or no lipid, supports this hypothesis. However, it is also possible that the cytosolic apoB-100 may exist in complex with additional cytosolic factors, because the density of apoB-100 has been previously suggested to increase when chaperones are bound to the particle (54). Immunofluorescence microscopy studies have shown that cytosolic apoB associates with lipid droplets, forming crescent-shaped structures (38) that represent the convergence between proteasomal and other degradation pathways.

Some aspects of the retrotranslocation of apoB-100 remain to be clarified. Investigations of the relative contributions of the chaperone proteins GRP78 (55), Hsp70, and Hsp90 (17) to the selection and retrotranslocation of apoB-100 are required. This may be particularly relevant because we observed a decrease in Hsp70 with si-p97 treatment. Furthermore, recently characterized components of the retrotranslocation machinery, such as Derlin-1, SVIP (56), VIMP (43), and UBX2 (57, 58), may also play regulatory roles in apoB degradation. We did not observe an effect of p97 knockdown on posttranslational stability beyond 1 h or on the secretion of apoB-100 from HepG2 cells. We also did not find a consistent increase in the mass of apoB-100 in the si-p97 cell membrane fraction after 3 days at reduced levels of p97. These observations may indicate that in the absence of p97, additional degradation mechanisms within the cell can still prevent the accumulation or secretion of incompletely assembled lipoprotein when ERAD is compromised.

In conclusion, evidence presented in this work suggests that p97 is a central component in retrotranslocation of apoB-100 for its delivery to the proteasome. Therefore, p97 may function at an early stage in apoB-100 biosynthesis where the presecretory fate of apoB is determined.

REFERENCES

1. Olofsson, S. O., L. Asp, and J. Boren. 1999. The assembly and secretion of apolipoprotein B-containing lipoproteins. *Curr. Opin. Lipidol.* **10:** 341–346.
2. Davidson, N. O., and G. S. Shelness. 2000. Apolipoprotein B: mRNA editing, lipoprotein assembly, and presecretory degradation. *Annu. Rev. Nutr.* **20:** 169–193.
3. Yao, Z., K. Tran, and R. S. McLeod. 1997. Intracellular degradation of newly synthesized apolipoprotein B. *J. Lipid Res.* **38:** 1937–1953.
4. Fisher, E. A., and H. N. Ginsberg. 2002. Complexity in the secretory pathway: the assembly and secretion of apolipoprotein B-containing lipoproteins. *J. Biol. Chem.* **277:** 17377–17380.
5. Yeung, S. J., S. H. Chen, and L. Chan. 1996. Ubiquitin-proteasome pathway mediates intracellular degradation of apolipoprotein B. *Biochemistry.* **35:** 13843–13848.
6. Qiu, W., R. Kohen-Avramoglu, F. Rashid-Kolvear, C. S. Au, T. M. Chong, G. F. Lewis, D. K. Trinh, R. C. Austin, R. Urade, and K. Adeli. 2004. Overexpression of the endoplasmic reticulum 60 protein ER-60 downregulates apoB100 secretion by inducing its intracellular degradation via a nonproteasomal pathway: evidence for an ER-60-mediated and pCMB-sensitive intracellular degradative pathway. *Biochemistry.* **43:** 4819–4831.
7. Cardozo, C., X. Wu, M. Pan, H. Wang, and E. A. Fisher. 2002. The inhibition of microsomal triglyceride transfer protein activity in rat hepatoma cells promotes proteasomal and nonproteasomal degradation of apoprotein B100. *Biochemistry.* **41:** 10105–10114.
8. Taghibiglou, C., D. Rudy, S. C. Van Iderstine, A. Aiton, D. Cavallo, R. Cheung, and K. Adeli. 2000. Intracellular mechanisms regulating apoB-containing lipoprotein assembly and secretion in primary hamster hepatocytes. *J. Lipid Res.* **41:** 499–513.
9. Pan, M., A. I. Cederbaum, Y. L. Zhang, H. N. Ginsberg, K. J. Williams, and E. A. Fisher. 2004. Lipid peroxidation and oxidant stress regu-

late hepatic apolipoprotein B degradation and VLDL production. *J. Clin. Invest.* **113:** 1277–1287.
10. Twisk, J., D. L. Gillian-Daniel, A. Tebon, L. Wang, P. H. Barrett, and A. D. Attie. 2000. The role of the LDL receptor in apolipoprotein B secretion. *J. Clin. Invest.* **105:** 521–532.
11. Liang, J. S., O. Distler, D. A. Cooper, H. Jamil, R. J. Deckelbaum, H. N. Ginsberg, and S. L. Sturley. 2001. HIV protease inhibitors protect apolipoprotein B from degradation by the proteasome: a potential mechanism for protease inhibitor-induced hyperlipidemia. *Nat. Med.* **7:** 1327–1331.
12. Schmidtke, G., H. G. Holzhutter, M. Bogyo, N. Kairies, M. Groll, R. de Giuli, S. Emch, and M. Groettrup. 1999. How an inhibitor of the HIV-I protease modulates proteasome activity. *J. Biol. Chem.* **274:** 35734–35740.
13. Goldberg, A. L. 2003. Protein degradation and protection against misfolded or damaged proteins. *Nature.* **426:** 895–899.
14. Voges, D., P. Zwickl, and W. Baumeister. 1999. The 26S proteasome: a molecular machine designed for controlled proteolysis. *Annu. Rev. Biochem.* **68:** 1015–1068.
15. Chuck, S. L., and V. R. Lingappa. 1992. Pause transfer: a topogenic sequence in apolipoprotein B mediates stopping and restarting of translocation. *Cell.* **68:** 9–21.
16. Du, E. Z., J. Kurth, S. L. Wang, P. Humiston, and R. A. Davis. 1994. Proteolysis-coupled secretion of the N terminus of apolipoprotein B. Characterization of a transient, translocation arrested intermediate. *J. Biol. Chem.* **269:** 24169–24176.
17. Gusarova, V., A. J. Caplan, J. L. Brodsky, and E. A. Fisher. 2001. Apoprotein B degradation is promoted by the molecular chaperones hsp90 and hsp70. *J. Biol. Chem.* **276:** 24891–24900.
18. Liang, J. S., T. Kim, S. Fang, J. Yamaguchi, A. M. Weissman, E. A. Fisher, and H. N. Ginsberg. 2003. Overexpression of the tumor autocrine motility factor receptor Gp78, a ubiquitin protein ligase, results in increased ubiquitinylation and decreased secretion of apolipoprotein B100 in HepG2 cells. *J. Biol. Chem.* **278:** 23984–23988.
19. Plemper, R. K., and D. H. Wolf. 1999. Retrograde protein translocation: ERADication of secretory proteins in health and disease. *Trends Biochem. Sci.* **24:** 266–270.
20. Meusser, B., C. Hirsch, E. Jarosch, and T. Sommer. 2005. ERAD: the long road to destruction. *Nat. Cell Biol.* **7:** 766–772.
21. Hiller, M. M., A. Finger, M. Schweiger, and D. H. Wolf. 1996. ER degradation of a misfolded luminal protein by the cytosolic ubiquitin-proteasome pathway. *Science.* **273:** 1725–1728.
22. Tsai, B., Y. Ye, and T. A. Rapoport. 2002. Retro-translocation of proteins from the endoplasmic reticulum into the cytosol. *Nat. Rev. Mol. Cell Biol.* **3:** 246–255.
23. Meyer, H. H., J. G. Shorter, J. Seemann, D. Pappin, and G. Warren. 2000. A complex of mammalian Ufd1 and Npl4 links the AAA-ATPase, p97, to ubiquitin and nuclear transport pathways. *EMBO J.* **19:** 2181–2192.
24. Ye, Y., H. H. Meyer, and T. A. Rapoport. 2003. Function of the p97-Ufd1-Npl4 complex in retrotranslocation from the ER to the cytosol: dual recognition of nonubiquitinated polypeptide segments and polyubiquitin chains. *J. Cell Biol.* **162:** 71–84.
25. Ye, Y., H. H. Meyer, and T. A. Rapoport. 2001. The AAA ATPase Cdc48/p97 and its partners transport proteins from the ER into the cytosol. *Nature.* **414:** 652–656.
26. Albring, J., J. O. Koopmann, G. J. Hammerling, and F. Momburg. 2004. Retrotranslocation of MHC class I heavy chain from the endoplasmic reticulum to the cytosol is dependent on ATP supply to the ER lumen. *Mol. Immunol.* **40:** 733–741.
27. Lapierre, L. R., D. L. Currie, Z. Yao, J. Wang, and R. S. McLeod. 2004. Amino acid sequences within the beta1 domain of human apolipoprotein B can mediate rapid intracellular degradation. *J. Lipid Res.* **45:** 366–377.
28. Cavallo, D., R. S. McLeod, D. Rudy, A. Aiton, Z. Yao, and K. Adeli. 1998. Intracellular translocation and stability of apolipoprotein B are inversely proportional to the length of the nascent polypeptide. *J. Biol. Chem.* **273:** 33397–33405.
29. McLeod, R. S., Y. Wang, S. Wang, A. Rusinol, P. Links, and Z. Yao. 1996. Apolipoprotein B sequence requirements for hepatic very low density lipoprotein assembly. Evidence that hydrophobic sequences within apolipoprotein B48 mediate lipid recruitment. *J. Biol. Chem.* **271:** 18445–18455.
30. Liao, W., B. H. Chang, M. Mancini, and L. Chan. 2003. Ubiquitin-dependent and -independent proteasomal degradation of apoB associated with endoplasmic reticulum and Golgi apparatus, respectively, in HepG2 cells. *J. Cell. Biochem.* **89:** 1019–1029.
31. Boren, J., S. Rustaeus, M. Wettesten, M. Andersson, A. Wiklund, and S. O. Olofsson. 1993. Influence of triacylglycerol biosynthesis rate on the assembly of apoB-100-containing lipoproteins in Hep G2 cells. *Arterioscler. Thromb.* **13:** 1743–1754.
32. Liao, W., X. Li, M. Mancini, and L. Chan. 2006. Proteasome inhibition induces differential heat shock protein response but not unfolded protein response in HepG2 cells. *J. Cell. Biochem.* **99:** 1085–1095.
33. Sakata, N., J. D. Stoops, and J. L. Dixon. 1999. Cytosolic components are required for proteasomal degradation of newly synthesized apolipoprotein B in permeabilized HepG2 cells. *J. Biol. Chem.* **274:** 17068–17074.
34. Wiertz, E. J., D. Tortorella, M. Bogyo, J. Yu, W. Mothes, T. R. Jones, T. A. Rapoport, and H. L. Ploegh. 1996. Sec61-mediated transfer of a membrane protein from the endoplasmic reticulum to the proteasome for destruction. *Nature.* **384:** 432–438.
35. Yu, H., G. Kaung, S. Kobayashi, and R. R. Kopito. 1997. Cytosolic degradation of T-cell receptor alpha chains by the proteasome. *J. Biol. Chem.* **272:** 20800–20804.
36. VanSlyke, J. K., and L. S. Musil. 2002. Dislocation and degradation from the ER are regulated by cytosolic stress. *J. Cell Biol.* **157:** 381–394.
37. Oberdorf, J., E. J. Carlson, and W. R. Skach. 2006. Uncoupling proteasome peptidase and ATPase activities results in cytosolic release of an ER polytopic protein. *J. Cell Sci.* **119:** 303–313.
38. Ohsaki, Y., J. Cheng, A. Fujita, T. Tokumoto, and T. Fujimoto. 2006. Cytoplasmic lipid droplets are sites of convergence of proteasomal and autophagic degradation of apolipoprotein B. *Mol. Biol. Cell.* **17:** 2674–2683.
39. Pariyarath, R., H. Wang, J. D. Aitchison, H. N. Ginsberg, W. J. Welch, A. E. Johnson, and E. A. Fisher. 2001. Co-translational interactions of apoprotein B with the ribosome and translocon during lipoprotein assembly or targeting to the proteasome. *J. Biol. Chem.* **276:** 541–550.
40. Mitchell, D. M., M. Zhou, R. Pariyarath, H. Wang, J. D. Aitchison, H. N. Ginsberg, and E. A. Fisher. 1998. Apoprotein B100 has a prolonged interaction with the translocon during which its lipidation and translocation change from dependence on the microsomal triglyceride transfer protein to independence. *Proc. Natl. Acad. Sci. USA.* **95:** 14733–14738.
41. Lee, R. J., C. W. Liu, C. Harty, A. A. McCracken, M. Latterich, K. Romisch, G. N. DeMartino, P. J. Thomas, and J. L. Brodsky. 2004. Uncoupling retro-translocation and degradation in the ER-associated degradation of a soluble protein. *EMBO J.* **23:** 2206–2215.
42. Bays, N. W., and R. Y. Hampton. 2002. Cdc48-Ufd1-Npl4: stuck in the middle with Ub. *Curr. Biol.* **12:** R366–R371.
43. Ye, Y., Y. Shibata, C. Yun, D. Ron, and T. A. Rapoport. 2004. A membrane protein complex mediates retro-translocation from the ER lumen into the cytosol. *Nature.* **429:** 841–847.
44. Flierman, D., Y. Ye, M. Dai, V. Chau, and T. A. Rapoport. 2003. Polyubiquitin serves as a recognition signal, rather than a ratcheting molecule, during retrotranslocation of proteins across the endoplasmic reticulum membrane. *J. Biol. Chem.* **278:** 34774–34782.
45. Zhou, M., E. A. Fisher, and H. N. Ginsberg. 1998. Regulated cotranslational ubiquitination of apolipoprotein B100. A new paradigm for proteasomal degradation of a secretory protein. *J. Biol. Chem.* **273:** 24649–24653.
46. Sakata, N., X. Wu, J. L. Dixon, and H. N. Ginsberg. 1993. Proteolysis and lipid-facilitated translocation are distinct but competitive processes that regulate secretion of apolipoprotein B in Hep G2 cells. *J. Biol. Chem.* **268:** 22967–22970.
47. Ota, T., C. Gayet, and H. N. Ginsberg. 2008. Inhibition of apolipoprotein B100 secretion by lipid-induced hepatic endoplasmic reticulum stress in rodents. *J. Clin. Invest.* **118:** 316–332.
48. Wojcik, C., M. Rowicka, A. Kudlicki, D. Nowis, E. McConnell, M. Kujawa, and G. N. DeMartino. 2006. Valosin-containing protein (p97) is a regulator of endoplasmic reticulum stress and of the degradation of N-end rule and ubiquitin-fusion degradation pathway substrates in mammalian cells. *Mol. Biol. Cell.* **17:** 4606–4618.
49. Alzayady, K. J., M. M. Panning, G. G. Kelley, and R. J. H. Wojcikiewicz. 2005. Involvement of the p97-Ufd1-Npl4 complex in the regulated endoplasmic reticulum-associated degradation of inositol 1,4,5-trisphosphate receptors. *J. Biol. Chem.* **280:** 34530–34537.
50. Baker, B. M., and D. Tortorella. 2007. Dislocation of an ER membrane glycoprotein involves the formation of partially dislocated ubiquitinated polypeptides. *J. Biol. Chem.* **282:** 26845–26856.
51. Zhong, X., Y. Shen, P. Ballar, A. Apostolou, R. Agami, and S. Fang. 2004. AAA ATPase p97/valosin-containing protein interacts with

gp78, a ubiquitin ligase for endoplasmic reticulum-associated degradation. *J. Biol. Chem.* **279:** 45676–45684.

52. Cao, J., J. Wang, W. Qi, H. H. Miao, J. Wang, L. Ge, R. A. Debose-Boyd, J. J. Tang, B. L. Li, and B. L. Song. 2007. Ufd1 is a cofactor of gp78 and plays a key role in cholesterol metabolism by regulating the stability of HMG-CoA reductase. *Cell Metab.* **6:** 115–128.
53. Adeli, K., J. Macri, A. Mohammadi, M. Kito, R. Urade, and D. Cavallo. 1997. Apolipoprotein B is intracellularly associated with an ER-60 protease homologue in HepG2 cells. *J. Biol. Chem.* **272:** 22489–22494.
54. Zhang, J., and H. Herscovitz. 2003. Nascent lipidated apolipoprotein B is transported to the Golgi as an incompletely folded intermediate as probed by its association with network of endoplasmic reticulum molecular chaperones, GRP94, ERp72, BiP, calreticulin, and cyclophilin B. *J. Biol. Chem.* **278:** 7459–7468.
55. Qiu, W., R. Kohen-Avramoglu, S. Mhapsekar, J. Tsai, R. C. Austin, and K. Adeli. 2005. Glucosamine-induced endoplasmic reticulum stress promotes ApoB100 degradation: evidence for Grp78-mediated targeting to proteasomal degradation. *Arterioscler. Thromb. Vasc. Biol.* **25:** 571–577.
56. Ballar, P., Y. Zhong, M. Nagahama, M. Tagaya, Y. Shen, and S. Fang. 2007. Identification of SVIP as an endogenous inhibitor of endoplasmic reticulum-associated degradation. *J. Biol. Chem.* **282:** 33908–33914.
57. Neuber, O., E. Jarosch, C. Volkwein, J. Walter, and T. Sommer. 2005. Ubx2 links the Cdc48 complex to ER-associated protein degradation. *Nat. Cell Biol.* **7:** 993–998.
58. Schuberth, C., and A. Buchberger. 2005. Membrane-bound Ubx2 recruits Cdc48 to ubiquitin ligases and their substrates to ensure efficient ER-associated protein degradation. *Nat. Cell Biol.* **7:** 999–1006.